

Evaluation of solar energetic Fe charge states: effect of proton-impact ionization

L. Kocharov¹, G.A. Kovaltsov^{1,2}, J. Torsti¹, and V.M. Ostryakov³

¹ Space Research Laboratory, Department of Physics, University of Turku, 20014 Turku, Finland

² Ioffe Physical-Technical Institute, St.Petersburg 194021, Russia

³ St.Petersburg State Technical University, St.Petersburg 195251, Russia

Received 16 December 1999 / Accepted 3 February 2000

Abstract. We present the energy-dependent rates of ionization and recombination of energetic Fe ions in solar coronal plasma for the energy range from 0.01 to above 100 MeV nucleon⁻¹. For the $> 0.1 \text{ MeV n}^{-1}$ ions, the energy dependencies become essential for both ionization and recombination processes. Ionization of the Fe projectile by ambient protons is important if the Fe energy exceeds typically 0.2–0.9 MeV n⁻¹. The equilibrium distributions established by the balance between ionization and recombination collisions are calculated for the temperature range $T = 10^6\text{--}10^7 \text{ K}$. We also present numerical calculations of the time-dependent (nonequilibrium) mean charge state at a given energy of the Fe ion. The results are relevant for the interpretation of charge states of the solar energetic ions. Our calculations support the qualitative conclusion that the observed energy-dependent Fe charge states are a result of concurrent acceleration and charge-changing processes. However, the estimated time scales of the processes are shorter than would be expected based on the energy-independent (thermal) charge-changing rates with no proton impact ionization included. The $\sim 30 \text{ MeV n}^{-1}$ Fe charge state observed in the 6–9 November 1997 event and our calculations suggest that the $\sim 30 \text{ MeV n}^{-1}$ ions were accelerated mainly near the Sun, at heliocentric distances $< 2R_{\odot}$.

Key words: Sun: corona – Sun: flares – Sun: particle emission – acceleration of particles

1. Introduction

If one wishes to probe the solar accelerator with solar energetic particles (SEPs), one is faced with a deficit of experimental data despite numerous observations in the interplanetary space. For this reason, the new observations of ionic charge states of SEPs are expected to provide crucial information on the acceleration sites. Brief but comprehensive reviews of the observations have been recently given by Barghouty & Mewaldt (1999) and by Reames (1999), so that we can refer an interested reader to those papers and references therein, and concentrate only on the relevant calculations applicable to the interpretation of the ob-

served Fe charge states. We choose Fe ions for the same reasons as Barghouty & Mewaldt (1999) did: iron charge states are expected to be quite sensitive to parameter variations because Fe should not be completely stripped even at rather high energies, and there is a set of atomic parameters needed to calculate all the charge states, as compiled by Arnaud & Raymond (1992). That is not to say that the charge-changing rates as given by Arnaud & Raymond (1992) for the thermal ions are directly applicable to energetic Fe projectiles. However many necessary atomic parameters could be extracted from that paper. Those parameters are used for evaluating *energy-dependent* ionization / recombination rates applicable to the energetic ions.

Luhn & Hovestadt (1987) gave examples of how charge-changing rates determined at thermal energies could be recalculated for energetic ions, but their calculations did not include Fe, being limited to elements from carbon through sulfur. Also the *proton-impact ionization* was missed. The latter however becomes important for solar energetic ions, because the velocity of the $\sim 1 \text{ MeV n}^{-1}$ ion is not less than the velocity of a thermal electron, and it is only the relative velocity of target and projectile that is important for a charge changing collision. The proton-impact ionization was also ignored in the Fe charge state calculations by Ruffolo (1997) and Barghouty & Mewaldt (1999). On the other hand, Kartavykh (1999) and Kartavykh & Ostryakov (1999) attempted to incorporate the ionization by the proton impact but essentially overestimated the corresponding cross section. However, it is known from atomic physics that (1) the cross section for ionization by a high-energy proton coincides with the electron cross section at equal velocities with respect to the atom/ion to be ionized (e.g. McDaniel 1989, his Eqs. 6-14-29 and 6-14-32); and (2) the threshold energy for the proton-impact ionization comes from the energy-time indeterminacy relation, so that $E_{\text{th}} \approx \frac{1}{4}(M_p/m_e)I$ (per nucleon), where M_p/m_e is the proton-to-electron mass ratio, and I is the ionization potential of the corresponding electron. For instance, the proton-impact ionization threshold for Fe⁺¹¹ is about 150 keV n^{-1} .

To the best of our knowledge, proton-impact ionization was firstly incorporated into SEP calculations by Kharchenko & Ostryakov (1987), being applied to helium and oxygen (also Ostryakov & Kharchenko 1988). Surprisingly, after the publica-

tions of Luhn & Hovestadt (1987) and Ostryakov & Kharchenko (1988) there was a degradation of the charge-changing rate performance, though the latter should be crucial for the accuracy of any charge-changing acceleration model. For this reason, we concentrate on the evaluation of the rate coefficients and on the most general estimates. The acceleration modeling should be the subject of a separate investigation, once the charge-changing rates have been established.

The organization of the present paper is as follows: Sect. 2 presents the evaluation of the energy-dependent ionization and recombination rates for Fe projectiles, including the proton-impact ionization. In Sect. 3, we apply the deduced rates to calculations of the equilibrium charge states of iron. We also calculate nonequilibrium charge states as a function of the electron density \times residence time product (Sect. 4). The implications and applications of our results are discussed in Sect. 5.

2. Ionization and recombination rates

A charge state distribution of energetic ions is established by the interplay of ionizing collisions and recombinations. Keeping in mind applications to particle acceleration modeling, we should start with a distribution function $N_i(E)$ for the ions of charge $Q = i - 1$ and kinetic energy E . We wish to calculate the ion fraction ϕ_i at a given energy

$$\phi_i = N_i(E) / \sum_{i=1}^k N_i(E), \quad \sum_{i=1}^k \phi_i = 1, \quad (1)$$

where k is the total number of charge states of a given chemical element ($k = 27$ for Fe). If one neglects acceleration, the balance of charge-changing processes is described by the following rate equations for ϕ_i (e.g., Luhn & Hovestadt 1987):

$$\begin{aligned} \frac{d\phi_1}{dt} &= n(-\phi_1 S_1 + \phi_2 \alpha_2), \\ \frac{d\phi_i}{dt} &= n(\phi_{i-1} S_{i-1} - \phi_i (S_i + \alpha_i) + \phi_{i+1} \alpha_{i+1}), \\ \frac{d\phi_k}{dt} &= n(\phi_{k-1} S_{k-1} - \phi_k \alpha_k), \end{aligned} \quad (2)$$

where n is the ambient electron number density; $S_i = S_i(T, E)$ is the temperature-energy-dependent ionization rate coefficient for transition from the ionization state i to the state $i + 1$; $\alpha_i = \alpha_i(T, E)$ is the recombination rate coefficient from the ionization state i to $i - 1$; S_i and α_i are in units of $\text{cm}^3 \text{s}^{-1}$. If acceleration is not omitted, one should start with a kinetic equation for $N_i(E)$ (e.g. Barghouty & Mewaldt 1999), where the same energy-dependent charge-changing rate coefficients should be employed. The rest of this section is devoted to a careful evaluation of the rate coefficients $S_i(T, E)$ and $\alpha_i(T, E)$ for a set of Fe ions.

2.1. Ionization rate coefficients

For an energetic Fe ion, the ionization rate comprises two parts corresponding to collisions with electrons S_e and collisions with ambient plasma protons and α -particles S_p ,

$$S = S_e + S_p, \quad (3)$$

where the charge state index i is omitted for brevity. The rate coefficients are obtained by integrating the corresponding cross section σ with a flux of ambient particles being considered in the rest frame of Fe. In particular, for electrons we have

$$S_e = \int_0^\infty \sigma_e(v) v f(v) dv, \quad (4)$$

where $f(v)$ is the electron velocity distribution in the rest frame of the Fe ion moving with velocity \mathbf{V} in respect to plasma. The distribution $f(v)$ is of the form parallel to expression (12) by Luhn & Hovestadt (1987):

$$f(v) = \frac{2}{\sqrt{\pi} v_T} \frac{v}{V} \exp\left(-\frac{v^2 + V^2}{v_T^2}\right) \sinh\left(\frac{2vV}{v_T^2}\right), \quad (5)$$

where

$$v_T = \sqrt{\frac{2k_B T}{m_e}} \quad (6)$$

is the thermal electron velocity. For a low velocity (e.g. thermal) Fe ion, $V \ll v_T$ and the electron distribution is a Maxwellian distribution independent of the ion energy E :

$$f(v) = \frac{4}{\sqrt{\pi} v_T^3} v^2 \exp\left(-\frac{v^2}{v_T^2}\right). \quad (7)$$

In the opposite case, $V \gg v_T$, the electron distribution does not depend on the plasma temperature:

$$f(v) = \delta(v - V), \quad (8)$$

and correspondingly

$$S_e = V \sigma_e(V). \quad (9)$$

A similar expression is always valid for the ionization rate due to energetic ion collisions with ambient protons and α -particles, because their thermal velocities are always small compared to V . Thus the sum of proton and helium impact ionization rates takes the form

$$S_p = R V \sigma_p(V), \quad (10)$$

where we have introduced a composition-dependent factor R normalizing the ionization rate to the electron number density n which appears in Eq. (2) (see also Sect. 2.1.2).

2.1.1. Ionization by electrons

The electron ionization cross section comprises the direct ionization part σ_c and the excitation autoionization part σ_a : $\sigma_e = \sigma_c + \sigma_a$. The conventional expressions for the electron cross sections are given by Arnaud & Raymond (1992, their Eqs. 1, 3). Given the cross sections, one can calculate the rate coefficients according to Eqs. (4, 5). For an ion with energy per nucleon E , the electron ionization coefficient is of the form

$$\begin{aligned} S_e = & \frac{2v_T}{\sqrt{\pi} k_B T} \frac{\exp(-y^2)}{y} \left[\int_{x_a}^\infty \Phi(u) \exp(-x^2) \sinh(2yx) dx + \right. \\ & \left. \sum_j \frac{1}{I_j} \int_{x_j}^\infty \Psi_j(u_j) \exp(-x^2) \sinh(2yx) dx \right], \end{aligned}$$

$$y = \frac{V}{v_T} = \sqrt{\frac{m_e E}{M_p k_B T}}, \quad u = \left(\frac{x}{x_a}\right)^2, \quad u_j = \left(\frac{x}{x_j}\right)^2, \\ x_a = \sqrt{\frac{I_a}{k_B T}}, \quad x_j = \sqrt{\frac{I_j}{k_B T}}, \quad (11)$$

where I_j is the ionization potential for electron level j of an Fe ion, and I_a is the excitation autoionization threshold. The summation is performed over the subshells j of the ion. Functions $\Psi_j(u_j)$ and $\Phi(u)$ come from the direct electron ionization cross section and from the excitation autoionization, respectively,

$$\Psi_j(u_j) = A_j \left(1 - \frac{1}{u_j}\right) + B_j \left(1 - \frac{1}{u_j}\right)^2 + C_j \ln(u_j) + D_j \frac{\ln(u_j)}{u_j}, \\ \Phi(u) = A + B \left(1 - \frac{1}{u}\right) + C \left(1 - \frac{1}{u^2}\right) + D \left(1 - \frac{1}{u^3}\right) + E_a \ln(u).$$

The two sets of numerical coefficients I_j , A_j , B_j , C_j , D_j , and I_a , A , B , C , D , E_a are given in Tables 1A and 1B respectively of Arnaud & Raymond (1992). We use the same designations as those by Arnaud & Raymond (1992), excluding E_a , which is identical to E in their Table 1B, and a shell index j is not explicit in their Table 1A.

Fig. 1 illustrates the electron impact ionization rate calculated for the ion Fe^{+17} in the energy range from $E = 10 \text{ keV n}^{-1}$ to 100 MeV n^{-1} . The asymptotes $V \ll v_T$ and $V \gg v_T$ are clearly seen. The former coincides with the result of Arnaud & Raymond (1992) for the thermal ions, while the latter coincides with Eq. (9). It is also seen that the region around 1 MeV n^{-1} , interesting for comparison with SEP observations, falls between the asymptotes.

2.1.2. Proton-impact ionization

In the general case of collision of a fully stripped ion with an atom or partially stripped ion, the electron-loss cross section comprises the charge-exchange part σ_{cx} and the ionization part σ_I , $\sigma_{\text{loss}} = \sigma_{\text{cx}} + \sigma_I$ (e.g., Janev 1983). However, in our case of collision of a proton with an already highly ionized Fe ion, there is no deep enough energy well near the proton to capture an Fe^{+n} electron, so that the charge-exchange is negligible and the impact ionization is the main process for the electron loss. The ionization process for very fast, fully stripped ions colliding with light atoms is well understood both theoretically (Bethe 1930, Inokuti 1978) and experimentally (e.g., Haugen et al. 1982). However, a precise description of the low energy, threshold behavior of σ_I should be based mainly on experimental data (cf. Janev 1994). The experimental data are not available for highly ionized Fe ions colliding with protons. No simple scaling applicable for all ions in the entire energy range is expected. For these reasons, we adopt here the conventional cross section published by Bohr (1948).

The Bohr cross section for the single ionization of an ion/atom by fast fully stripped ions of charge Z and velocity V can be expressed in the form (Knudsen et al. 1984)

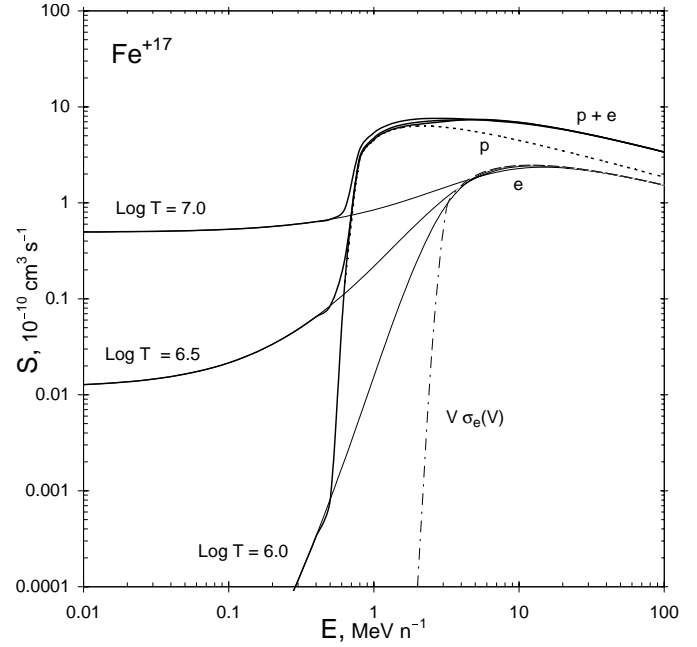


Fig. 1. Ionization rate coefficients for the ion Fe^{+17} . Thin curves illustrate the electron contribution S_e ; the dash-dotted line represents its high-energy asymptote. The dotted line p illustrates the proton and α -particle impact ionization S_p . Total ionization rates are shown with heavy solid curves

$$\sigma_I = 4\pi a_o^2 Z^2 \frac{I_o}{I} \left(\frac{v_o}{V}\right)^2 F(\eta, \kappa), \quad (12)$$

where I is the ionization potential of an ionic/atomic electron; $I_o = 13.6 \text{ eV}$; $v_o = 2.189 \times 10^8 \text{ cm s}^{-1}$ is the Bohr velocity, and $a_o = 5.292 \times 10^{-9} \text{ cm}$ is the Bohr radius. The theoretical treatment of ionization depends on the values of two dimensionless parameters η and κ ,

$$\eta = \frac{2V}{v_I}, \quad \kappa = \frac{2Zv_o}{V}, \quad (13)$$

where $v_I = v_o \sqrt{I/I_o}$. The resulting parameter dependencies can be reduced to the compact form of the function $F(\eta, \kappa)$,

$$F(\eta, \kappa) = \left[\left(\left[\frac{\kappa}{\eta} \right]^{-1} + \delta \ln \left[\frac{\eta^2}{[\kappa]^2} \right] - \frac{1}{\eta^2} \right) + 1 \right] - 1, \quad (14)$$

where parameter δ is a fraction of distant (small momentum transfer) encounters leading to ionization. The square brackets in Eq. (14) have the property: $[x] = x$ for $x > 1$, $[x] = 1$ for $x \leq 1$.

We consider ionization by the fully stripped ions, protons or α -particles of energy per nucleon E and charge $Z = 1$ or 2 , respectively. Expression (14) is compact but actually not very simple. For this reason, after some reduction, introducing two new parameters

$$u = \frac{m_e E}{M_p I} \quad \text{and} \quad \kappa_o = \frac{4Z}{\sqrt{I/I_o}}, \quad (15)$$

we recast expression (12) also in a more explicit form

$$\sigma_I = 4\pi a_o^2 Z^2 \left(\frac{I_o}{I}\right)^2 \frac{1}{u} F_1(u, \kappa_o), \quad (16)$$

where $F_1(u, \kappa_o)$ is defined as following

1. In the case of $\kappa_o \leq 1$ (it means $I \geq 16Z^2I_o$),

$$F_1 = 1 - \frac{1}{4u} + \delta \ln(4u) \quad \text{at } u > 1/4, \quad (17)$$

$$F_1 = 0 \quad \text{at } u \leq 1/4. \quad (18)$$

2. In the case of $\kappa_o > 1$ (it means $I < 16Z^2I_o$),

$$F_1 = 1 - \frac{1}{4u} + \delta \ln(4u) \quad \text{at } u > \kappa_o^2/4, \quad (19)$$

$$F_1 = 1 - \frac{1}{4u} + \delta \ln\left(\frac{16u^2}{\kappa_o^2}\right) \quad \text{at } \kappa_o/4 < u \leq \kappa_o^2/4, \quad (20)$$

$$F_1 = \frac{4u}{\kappa_o} - \frac{1}{4u} \quad \text{at } \sqrt{\kappa_o}/4 < u \leq \kappa_o/4, \quad (21)$$

$$F_1 = 0 \quad \text{at } u \leq \sqrt{\kappa_o}/4. \quad (22)$$

If the charge of ionizing particle Z is not very high, as our $Z = 1$ or 2 , and iron is already highly ionized, the case 1 works and the ionization threshold energy is exactly equal to $\frac{1}{4}(M_p/m_e)I$.

A total proton ionization cross section, σ_p , is a sum of the cross sections (16) over all electrons of an Fe ion:

$$\sigma_p = \sum_j n_j \sigma_I(I = I_j), \quad (23)$$

where j is the index of the electron subshell with the ionization potential I_j , and the number of electrons in the subshell is n_j .

We still have to refine two last points: (i) the parameter δ is estimated to be ~ 0.3 , but its precise value for Fe ions is not known; and (ii) the high-velocity asymptote of the proton impact cross section σ_I as adopted by Knudsen et al. (1984) may not exactly coincide with the asymptote of the electron impact cross section published by Arnaud & Raymond (1992). For the purpose of removing uncertainty in the value of δ and getting consistency between the proton and electron cross sections, we introduce a normalization factor to the proton cross section: $\sigma_I \leftarrow A_{\text{norm}} \sigma_I$, where the factor A_{norm} is expected to be close to unity. Then we set the high-velocity asymptote of the proton cross section equal to the high-velocity asymptote of the electron direct ionization cross section. Skipping some algebra, we give the resulting values of the parameters

$$\delta = \frac{C_j}{A_j + B_j - C_j \ln 4}, \quad A_{\text{norm}} = \frac{A_j + B_j - C_j \ln 4}{4\pi a_o^2 I_o^2 n_j}, \quad (24)$$

where coefficients A_j , B_j and C_j are the same as in Sect. 2.1.1. The deduced sets of δ and A_{norm} are typified by values of ≈ 0.3 and ≈ 0.9 , respectively. Finally, for all Fe-charge states $\geq +8$ ($I_j \geq 16I_o = 218 \text{ eV}$, $\kappa_o \leq 1$), the proton impact ionization cross section takes the form of

$$\sigma_p(E) = \sum_j \frac{1}{u_j I_j^2} \left((A_j + B_j - C_j \ln 4) \left(1 - \frac{1}{4u_j}\right) + C_j \ln(4u_j) \right),$$

$$u_j = \frac{m_e E}{M_p I_j}. \quad (25)$$

A contribution of α -particles is approximately accounted for by a factor R :

$$R = \frac{n_{\text{H}} + Z_{\text{He}}^2 n_{\text{He}}}{n}, \quad (26)$$

where the electron density $n = n_{\text{H}} + Z_{\text{He}} n_{\text{He}}$, $Z_{\text{He}} = 2$. At $n_{\text{He}}/n_{\text{H}} = 0.08$ (Grevesse & Sauval 1998), this yields

$$R = \frac{1 + 4n_{\text{He}}/n_{\text{H}}}{1 + 2n_{\text{He}}/n_{\text{H}}} = 1.14, \quad (27)$$

the value actually adopted in the ionization rate expression (10). The sum of proton and α -particle impact ionizations is shown as a dotted line in Fig. 1.

2.2. Recombination rate coefficients

It is well known that an ion recombination rate comprises two terms,

$$\alpha = \alpha_r + \alpha_d, \quad (28)$$

corresponding to radiative (subscript r) and dielectronic (subscript d) recombination. Each rate should be obtained by convolving the corresponding cross section with the ambient electron distribution as seen in the rest frame of the Fe ion (Eq. 5):

$$\alpha_{r(d)} = \int_0^\infty \sigma_{r(d)}(v) v f(v) dv. \quad (29)$$

In the general case, these rates depend on both the ambient electron temperature and the Fe ion energy. However, in the low energy (thermal) limit, the energy dependence disappears (see Eq. 7), and the recombination rate coincides with the known thermal recombination rate: $\alpha_{r(d)} = \alpha_{r(d)}^T(T)$.

Following Luhn & Hovestadt (1987), we adopt a simplified expression for the radiative recombination cross section (their Eq. 6),

$$\sigma_r(E_e) = C_r E_e^{-a}. \quad (30)$$

The parameters C_r and a are selected to fit the recombination rates previously established for thermal ions. Evaluating integral (29) in the thermal limit yields

$$\alpha_r^T = \frac{2}{\sqrt{\pi}} v_T C_r (k_B T)^{-a} \Gamma(2-a). \quad (31)$$

Then, for the accelerated ion of energy per nucleon E , the recombination coefficient can be expressed in terms of α_r^T as

$$\alpha_r = \alpha_r^T \frac{1}{\Gamma(2-a)} \frac{\exp(-y^2)}{y} \int_0^\infty x^p \exp(-x^2) \sinh(2xy) dx,$$

where $p = 2(1-a)$, $\Gamma(x)$ is the gamma function,

$$y = \frac{V}{v_T} = \sqrt{\frac{m_e E}{M_p k_B T}}. \quad (32)$$

In our calculations we use α_r^T in the form of Eq. (4) by Shull & Steenberg (1982)

$$\alpha_r^T = A_r \left(\frac{T}{10^4 \text{K}} \right)^{-x_r}, \quad (33)$$

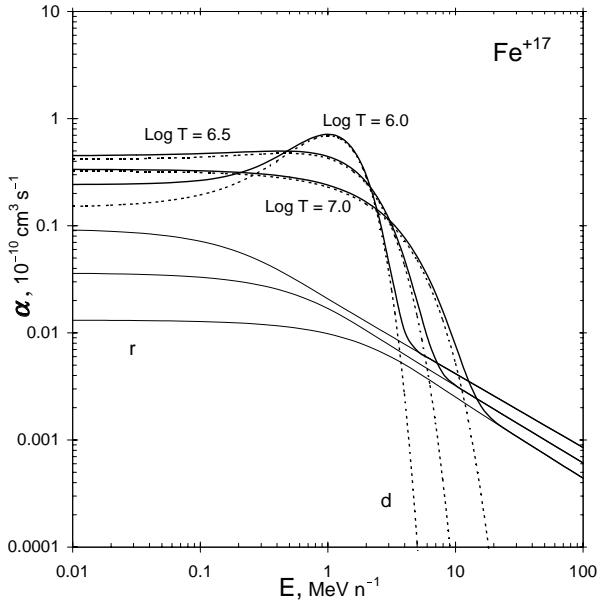


Fig. 2. Recombination rates for Fe^{+17} . Thin lines r illustrate contribution of the radiative recombination; dotted lines d represent the dielectronic recombination. The total recombination rates are shown by heavy solid lines labeled with the corresponding temperatures

and correspondingly $a = \chi_r + 0.5$. For $\text{Fe}^{+14} - \text{Fe}^{+25}$ ions, we adopt χ_r in the form of expression (6) by Arnaud & Raymond (1992), $\chi_r = \alpha + \beta \log(T/10^4 \text{K})$, and Table 2 therein for values A_r , α and β . For $\text{Fe}^0 - \text{Fe}^{+13}$ and Fe^{+26} ions, the values of A_r and $\chi_r = \text{constant}_T$ are published by Shull & Steenberg (1982) (their Table 2 and errata).

The cross section for the dielectronic recombination is in the form (e.g. Luhn & Hovestadt 1987)

$$\sigma_d(E_e) = \sum_j \sigma_{d,j} \delta(E_e - E_j). \quad (34)$$

The quantity $\sigma_{d,j}$ is a constant which gives the strength of the contribution of level j with energy E_j into recombination of the ambient electron of energy E_e . Substituting expressions (7) and (34) into (29) and integrating yield the thermal dielectronic recombination coefficient, α_d^T , for the electron Maxwellian distribution of temperature T

$$\alpha_d^T = \sum_j \alpha_{d,j}^T, \quad (35)$$

$$\alpha_{d,j}^T = \frac{4}{\sqrt{2\pi m_e k_B T}} \sigma_{d,j} \frac{E_j}{k_B T} \exp\left(-\frac{E_j}{k_B T}\right).$$

Similar to the radiative recombination, we express the dielectronic recombination rate for an accelerated ion of energy E in terms of the thermal dielectronic recombination rate:

$$\alpha_d = \sum_j \alpha_{d,j}^T \frac{\sinh(2x_j y)}{2x_j y} \exp(-y^2), \quad (36)$$

where

$$y = \frac{V}{v_T} = \sqrt{\frac{m_e E}{M_p k_B T}}, \quad x_j = \sqrt{\frac{E_j}{k_B T}}. \quad (37)$$

In our calculations we use the expression for $\alpha_{d,j}^T$ from Arnaud & Raymond (1992) (their Eq. 7),

$$\alpha_{d,j}^T = c_j T^{-3/2} \exp\left(-\frac{E_j}{k_B T}\right), \quad (38)$$

and the values of c_j and E_j for the Fe ions from their Table 3.

Fig. 2 illustrates the recombination rate calculated for the ion Fe^{+17} in the energy range from $E = 10 \text{ keV n}^{-1}$ to 100 MeV n^{-1} . It is seen that the energy dependence of the recombination should not be neglected for SEPs with energy $> 0.1 \text{ MeV n}^{-1}$.

3. Equilibrium charges of energetic ions

Given a set of charge changing rates, one can calculate charge state distributions of the energetic Fe ions in a variety of acceleration / propagation models. We start with a simple calculation of the steady state charges of Fe ions after passing through a coronal plasma with all energy change effects neglected. We believe that such a simple calculation is useful for estimates and should precede incorporation of the rates into the more sophisticated computations. For the equilibrium case, Eq. (2) is reduced to

$$\phi_i S_i = \phi_{i+1} \alpha_{i+1}. \quad (39)$$

A solution of the set of Eqs. (1, 39) can be written in the form

$$\phi_i = \Pi_i \Sigma^{-1}, \quad (40)$$

where

$$\Pi_i = \left(\prod_{j=1}^{i-1} S_j \right) \left(\prod_{j=i}^{k-1} \alpha_{j+1} \right), \quad i = 2, 3 \dots k-1;$$

$$\Pi_1 = \prod_{j=1}^{k-1} \alpha_{j+1}, \quad \Pi_k = \prod_{j=1}^{k-1} S_j, \quad \Sigma = \sum_{i=1}^k \Pi_i. \quad (41)$$

In Fig. 3 we show the equilibrium mean charge of Fe as a function of its kinetic energy for eleven values of the electron temperature from $1 \times 10^6 \text{ K}$ through $1 \times 10^7 \text{ K}$. The effect of the proton-impact ionization is illustrated in Fig. 4. It is seen that inclusion of the proton ionization essentially increases the mean charge of an accelerated Fe ion in the SEP energy range. At $E > 150 \text{ keV n}^{-1}$, the equilibrium charge is ruled mainly by the proton-impact ionization, and the mean charge \bar{Q} could be estimated using the equation: $I(\bar{Q}) = 4m_e E / M_p$, where $I(\bar{Q})$ is the ionization potential for the ion $\text{Fe}^{+\bar{Q}}$, E is the energy per nucleon. Fig. 5 shows fractions of different Fe ions contributing to the mean charge in a wide energy range, from 10 keV n^{-1} , where ionization is nearly thermal, to SEP energies, where the Fe ions should be highly stripped.

4. Nonequilibrium calculations

Observations of the intermediate charge states of energetic ions, between the thermal ionization and the equilibrium ionization \bar{Q} , could be a signature of nonequilibrium ionization during either SEP acceleration or transport or both. To calculate a

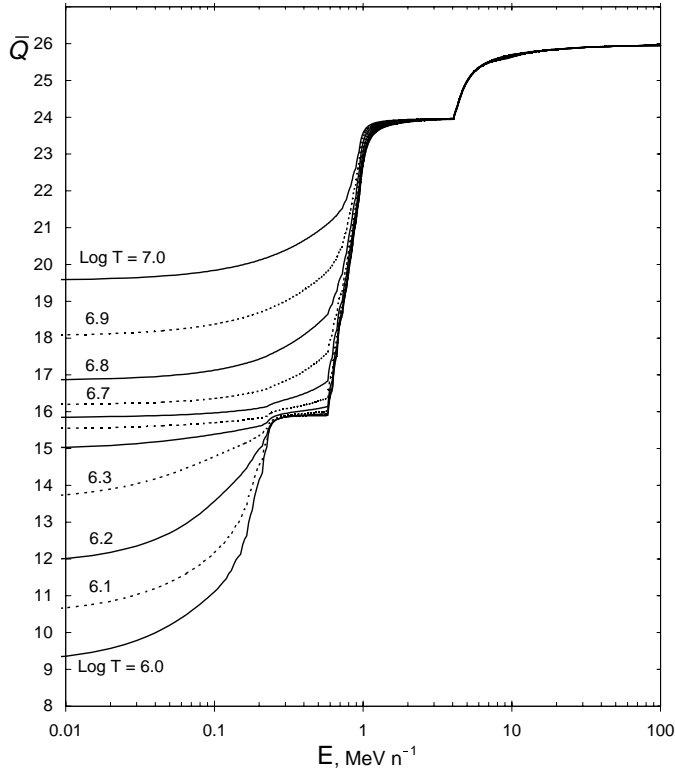


Fig. 3. The equilibrium mean charge of Fe as a function of its kinetic energy. The parameter next to the curves gives the logarithm of the ambient plasma electron temperature

nonequilibrium charge state, we solve Eqs. (1, 2) with a Monte Carlo method. This method is employed because we actually incorporated the charge changing processes into an available Monte Carlo code for ion acceleration. However, for the goals of the present paper, the acceleration has been turned off and ions are removed from the system after a fixed time has elapsed. Thus we present results of calculations of the nonequilibrium charge distributions for the Fe ions with a constant energy E but a variable charge Q depending on the time t that particles have spent in the region of the electron density n . Such a distribution does not depend on details of acceleration / transport models and could be employed for a qualitative analysis of experimental data and estimates.

In Fig. 6, we show the calculated nonequilibrium mean charges $\langle Q \rangle$ for energetic ions injected with the initial charge $Q_0 = +11$ in the plasma of temperature $T = 1.6 \times 10^6$ K. The time profiles reveal no universal, energy independent time scale for the charge change. A time scale for leaving the initial (thermal) charge varies from $\sim 3 \times 10^8 \text{ cm}^{-3} \text{ s}$ to $\sim 10^{10} \text{ cm}^{-3} \text{ s}$ depending on energy. Equilibrium charge is approached on a time scale from $\sim 10^{10} \text{ cm}^{-3} \text{ s}$ to $\sim 10^{11} \text{ cm}^{-3} \text{ s}$.

Fig. 7 shows the temperature dependence of the time profiles of the mean charge, $\langle Q \rangle$. The initial rise of $\langle Q \rangle$ is not sensitive to the electron temperature because ionization is mainly due to collisions with protons, and recombination is not essential as long as $\langle Q \rangle$ is far from its equilibrium value, \bar{Q} . A dependence on the initial charge Q_0 is illustrated in Fig. 8. It is noteworthy

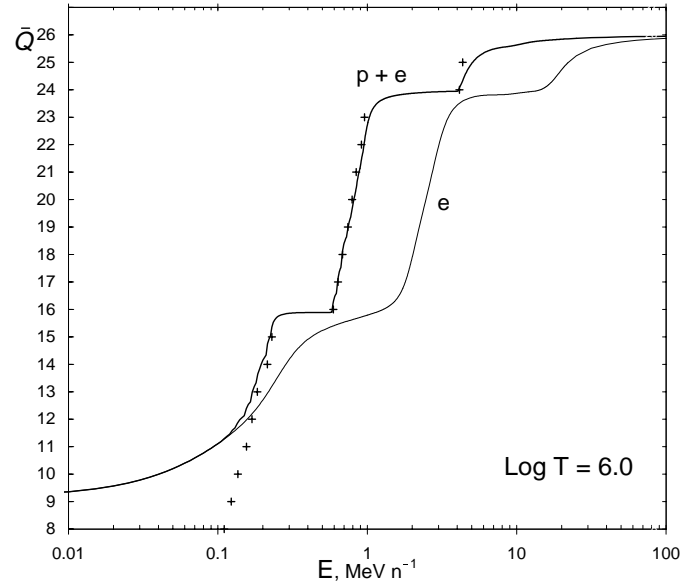


Fig. 4. Illustration of the effect of proton-impact ionization on the equilibrium mean charge of energetic Fe ions, \bar{Q} . The thin curve e represents \bar{Q} calculated without inclusion of proton impact ionization. Crosses depict points where the ionization potential obeys the equation $I(\bar{Q}) = (4m_e/M_p)E$

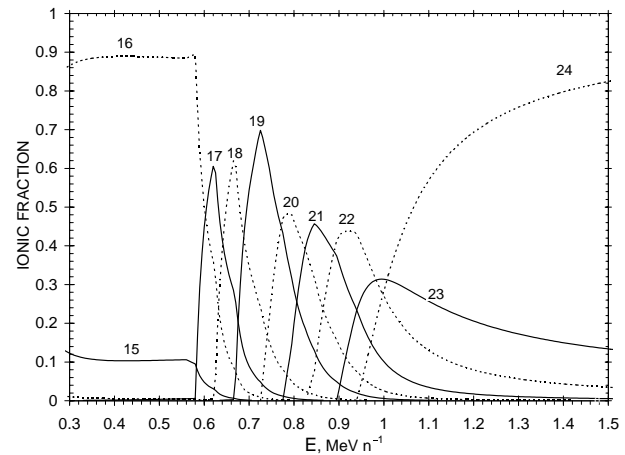
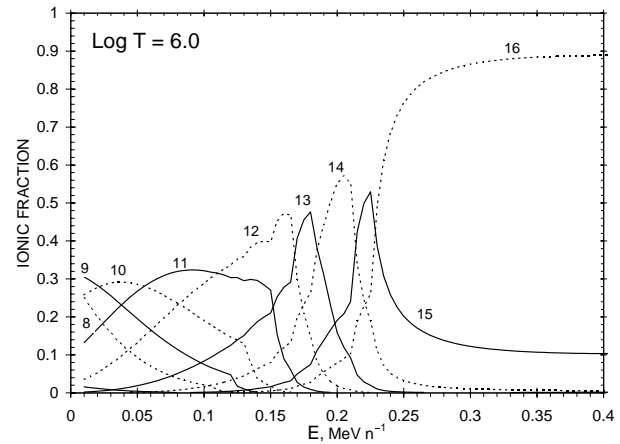


Fig. 5. The equilibrium ionic fraction of energetic Fe vs. kinetic energy per nucleon. The parameter next to the curves is the ion charge Q

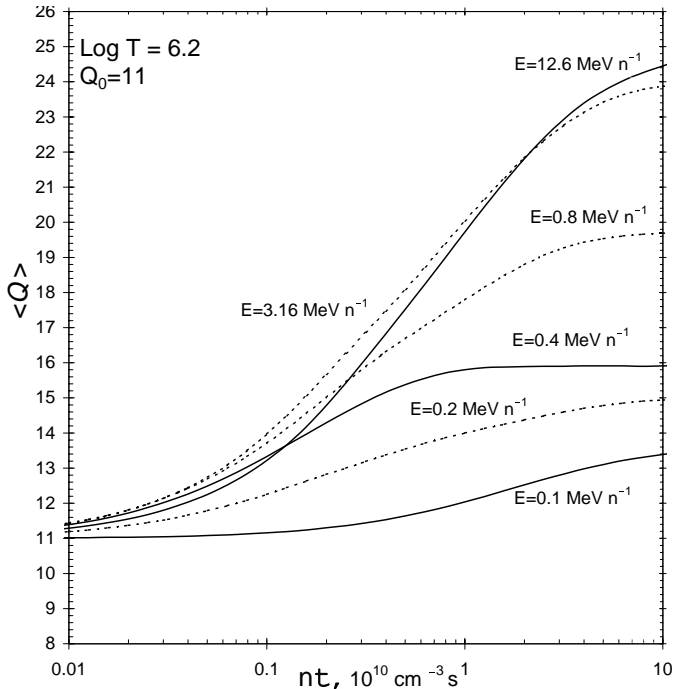


Fig. 6. The nonequilibrium mean charge as a function of time for different values of the Fe ion energy E . The initial ion charge is $Q_0 = +11$

that it takes one order of magnitude longer time to approach the equilibrium charge \bar{Q} from a higher value of the initial charge, $Q_0 > \bar{Q}$, than to approach \bar{Q} from $Q_0 < \bar{Q}$, because the recombination is relatively slow.

5. Discussion

The initial charge state of Fe ions is believed to be a “thermal” charge state calculated for optically thin coronal plasma, e.g. by Arnoud & Raymond (1992). During ion acceleration and/or transport, the initial charge may be changed. The mean charge of Fe ions was recently observed to increase with energy from ~ 0.2 to $\sim 40 \text{ MeV n}^{-1}$ (Oetliker et al. 1997, Möbius et al. 1999, Mazur et al. 1999, Cohen et al. 1999). Such an energy-dependent feature may come from the charge-changing processes during an acceleration (Kurganov & Ostryakov 1991, Ostryakov & Stovpyuk 1997, Barghouty & Mewaldt 1999), suggesting that the coronal + interplanetary transport is fast and does not alter the accelerated ion charge state. Alternatively, it might be suggested that energetic particles spend ~ 1 day trapped behind an interplanetary shock sampling the densities at several solar radii, and their charge might tend to the equilibrium charge state appropriate for their velocity through the material (Reames 1999). It might also be suggested that acceleration is very fast, not changing an initial charge state, but takes place close to Sun, and ions may be partially stripped during passage through the overlying coronal layers.

To discriminate between those alternatives, we use the nonequilibrium charge calculations of Sect. 4. We employ the energy-dependent Fe charge states observed after the 6 November 1997 flare (Möbius et al. 1999, Cohen et al. 1999) and our

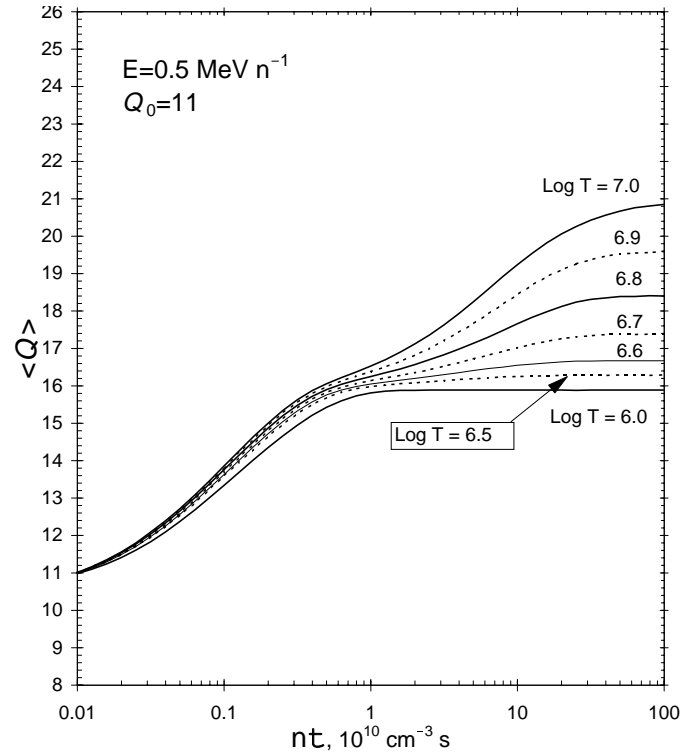


Fig. 7. The nonequilibrium mean charge vs. time for different values of the ambient plasma temperature T . The initial ion charge is $Q_0 = +11$, the kinetic energy being 0.5 MeV n^{-1}

calculations shown in Fig. 6. The reported charge states fall between the “thermal” charge states and the equilibrium mean charges \bar{Q} shown in Fig. 3. This indicates that the observed charges are of a nonequilibrium nature. The experimental data were originally plotted on the charge-energy, $\langle Q \rangle - E$, plane. In Fig. 9 we map the data onto the $n \times t - E$ plane, in which t is the residence time in the region of plasma density n . The points in the figure depict the time required for stripping the ion Fe^{+11} to the observed charge state at a given energy E . It is seen that the residence time for ion stripping (or $n \times t$) turns out to be a rising function of energy. However, we do not expect that the transport time of a higher energy ion is longer than that of a lower energy one. For this reason, we can rule out both transport type explanations, that due to a direct passage through the dense coronal layers and that due to a long-time trapping behind the interplanetary shock. Thus we are left with the charge-changing acceleration suggested by Barghouty & Mewaldt (1999), because on average it takes an ion a longer time to be accelerated to a higher energy, so that the $n \times t$ product should gradually rise with increasing energy if concurrent charge changing and acceleration processes take place. However, the rise is not expected to be very steep. Our calculations support the qualitative conclusion of Barghouty & Mewaldt (1999), but the numerical results are very different, partly due to the fact that our charge-changing rates also account for the proton-impact ionization. The proton-impact ionization was incorporated into the recent calculations of the Fe charge states performed by Kar-

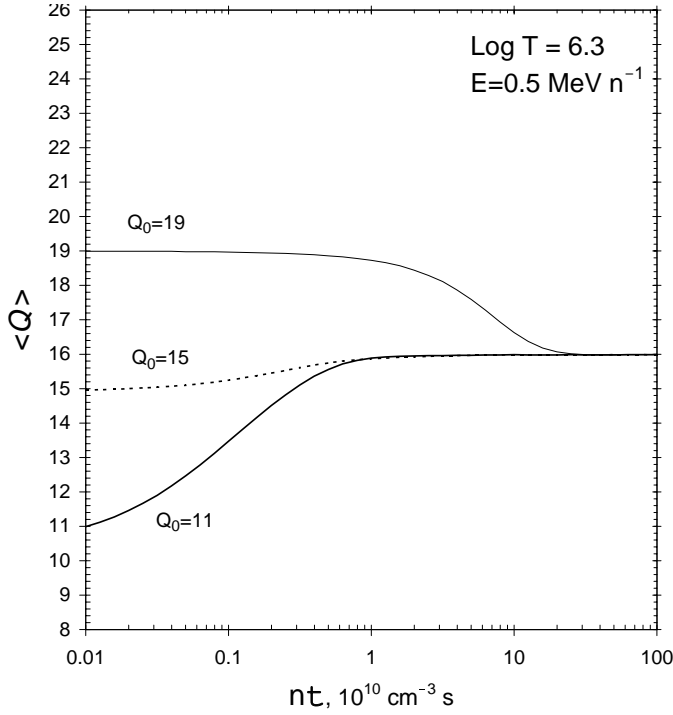


Fig. 8. The nonequilibrium mean charge as a function of time for different initial charge states Q_0

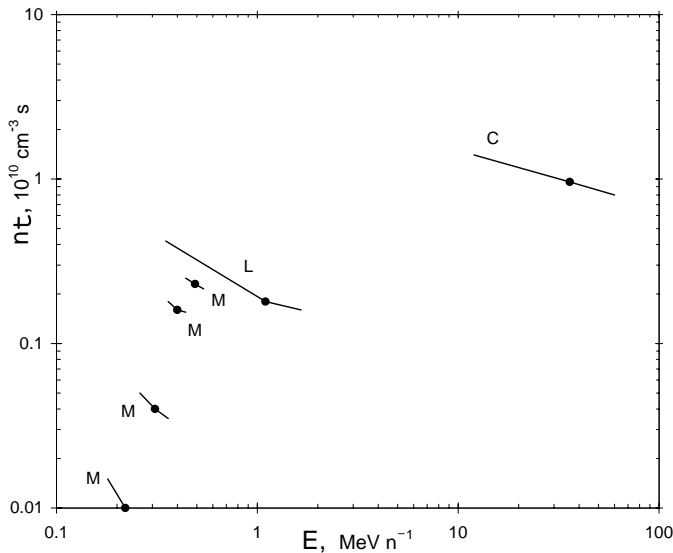


Fig. 9. The observed mean charge states (points and experimental error bars) mapped onto the electron density \times time product axis vs. energy. Labels next to the points correspond to the Fe charge states reported by Möbius et al. (1999) and Cohen et al. (1999) for the 6–9 November 1997 event (labels M and C, respectively) and by Luhn et al. (1984) for three other events (label L)

tavykh (1999) (also Kartavykh & Ostryakov 1999). However, the proton-impact ionization rate of Fe ions was essentially overestimated because of a misinterpretation of the atomic physics results published by Sidorovich & Nikolaev (1988) (also Nikolaev & Sidorovich 1989). We employ presently conventional

proton-impact ionization cross section, but because of a lack of experimental data, further studies of the cross-section threshold behavior are still desirable.

It is seen from Fig. 9 that for the $\sim 30 \text{ MeV n}^{-1}$ ions the product $n \times t$ is estimated to be $\approx 10^{10} \text{ cm}^{-3} \text{ s}$. In a general way, the characteristic time scale increases and density decreases with increasing distance from the Sun. We express the residence time in terms of the acceleration region depth L and a bulk velocity U (see e.g. Drury et al. 1999), so that $n \times t = n \times L/U$. At nearly constant U (e.g. estimated as Alfvén velocity) the $n \times t$ product definitely decreases with increasing distance from the Sun. The value $n \times t = 10^{10} \text{ cm}^{-3} \text{ s}$ could be achieved at $L = 0.3 R_{\odot}$, $U = 6 \times 10^7 \text{ cm s}^{-1}$ and $n = 3 \times 10^7 \text{ cm}^{-3}$. That means that $\sim 30 \text{ MeV n}^{-1}$ ions were accelerated at heliocentric distances $< 2R_{\odot}$. A slow decrease of $n \times t$ with decreasing energy from ~ 30 to $\sim 1 \text{ MeV n}^{-1}$ can be naturally explained as due to the concurrent acceleration and charge changing processes. However, the decrease below 1 MeV n^{-1} is much steeper. It indicates that a second effect should also be involved. The low-energy (sub MeV n^{-1}) ions seem to be accelerated farther from the Sun when the shock travels in the interplanetary medium, as Reames (1999) proposed.

Acknowledgements. The study was supported by the Academy of Finland and partially by the Russian Foundation of Basic Research (grants 00-02-17031 and 99-02-18398).

References

- Arnaud M., Raymond J. 1992, *ApJ* 398, 394
 Barghouty A.F., Mewaldt R.A. 1999, *ApJ* 520, L127
 Bethe H. 1930, *Ann. Phys.* 5, 325
 Bohr N. 1948, *K. Danske Vidensk. Selsk., Mat.-Fys. Meddr.* 18, no 8
 Cohen C.M.S., Cummings A.C., Leske R.A., et al. 1999, *Geophys. Res. Lett.* 26, NO.2, 149
 Drury L.O’C., Duffy P., Eichler D., et al. 1999, *A&A* 347, 370
 Grevesse N., Sauval A.J. 1998, *Space Sci. Rev.* 85, 161
 Haugen H.K., Andersen L.H., Hvelplund P., et al. 1982, *Phys. Rev. A* 26, 1950
 Inokuti M. 1978, *Rev. Mod. Phys.* 50, 23
 Janev R.K. 1983, *Phys. Rev. A* 28, 1810
 Janev R.K. 1994, *Phys. Rev. A* 49, R645
 Kartavykh Yu.Yu. 1999, Thesis “Stochastic Acceleration of Heavy Ions in Solar Flares: Coulomb Losses and Charge Change”, Pulkovo Observatory, St.Petersburg, 123 p.
 Kartavykh Yu.Yu., Ostryakov V.M. 1999, *Proc. 26th Internat. Cosmic Ray Conf., Salt Lake City*, 6, 272
 Kharchenko A.A., Ostryakov V.M. 1987, *Proc 20th Internat. Cosmic Ray Conf., Moscow*, 3, 248
 Knudsen H., Andersen L.H., Hvelplund P., et al. 1984, *J. Phys. B: At. Mol. Phys.* 17, 3545
 Kurganov I.G., Ostryakov V.M. 1991, *Soviet Astron. Lett.* 17, NO.2, 177
 Luhn A., Hovestadt D. 1987, *ApJ* 317, 852
 Luhn A., Klecker B., Hovestadt D., et al. 1984, *Adv. Space Res.* 4, 161
 McDaniel E.W. 1989, *Atomic collisions*, Wiley, New York, p. 432
 Mazur J.E., Mason G.M., Loofer M.D., et al. 1999, *Geophys. Res. Lett.* 26, NO.2, 173
 Möbius E., Popecki M., Klecker B., et al. 1999, *Geophys. Res. Lett.* 26, NO.2, 145

- Nikolaev V.S., Sidorovich V.A. 1989, Nucl. Instrum. and Methods in Phys. Res. B36, 239
- Oetliker M., Klecker B., Hovestadt D., et al. 1997, ApJ 477, 495
- Ostryakov V.M., Kharchenko A.A. 1988, Bulletin of the Academy of Sciences of the USSR 52, NO.12, 109
- Ostryakov V.M., Stovpyuk M.F. 1997, Astronomy Reports 41, NO.3, 386
- Ruffolo D. 1997, ApJ 481, L119
- Reames D.V. 1999, Space Sci. Rev. 90, 413
- Sidorovich V.A., Nikolaev V.S. 1988, In: Berényi D., Hock G. (eds.) Lecture Notes in Physics 294, Proc. 3rd Workshop on High-Energy Ion-Atom Collisions, Springer-Verlag, Berlin, p.437
- Shull J.M., Steenberg M.V. 1982, ApJS 48, 95; Errata 49, 351